International Journal of Thermodynamics (IJoT)
ISSN 1301-9724 / e-ISSN 2146-1511
https://dergipark.org.tr/en/pub/ijot

Vol. 25 (No. 2), pp. 064-075, 2022
doi: 10.5541/ijot.1017374
Published online: June 1, 2022

A Residual Thermodynamic Analysis of Turbulence – Part 2: Pipe Flow Computations and Further Development of Theory

M. Gustavsson*

Hot Disk AB, c/o Chalmers Science Park, Sven Hultins Gata 9, SE-41288 Gothenburg, Sweden
E-mail: Mattias.Gustavsson@hotdiskinstruments.com

Received 1 November 2021, Revised 14 March 2022, Accepted 24 March 2022

Abstract

Single-phase turbulent pipe flows are analysed utilizing a new theory presented in a parallel paper. Arguably this new theory implies improvements in matching modelling results with experimental observations: To illustrate, unique for these computations is that a 1st law balance agreement between simulations and corresponding experiments is achieved, while resolving the time-averaged fluid flow velocity (including the various inner turbulent zones) and accounting for the wall surface roughness. Testing this new approach, the computations of 20 cases of turbulent pipe flow arrives at a remarkably high amount of kinetic energy dissipation occurring at near-wall positions, where some 54-83% of the net kinetic energy dissipation occurs within the viscous sublayer-, and 17-39% within the buffer layer. Although turbulence incorporates time-varying phenomena, *e.g.* swirls, large eddies, and breakup of the latter, it is argued that simulating these would have practically no effect on the net kinetic energy dissipation – and the associated wall shear stress – for the present pipe flow cases. Another illustration of the improvements relate to transition computations: While a proposed nominal transition model arrives at fair values of transition Reynolds numbers, some improvements on this transition analysis can be made, *e.g.* allowing for the modelling of the turbulence onset/offset hysteresis behaviour. For scientists who wish to model time-varying phenomena, *e.g.* for the study of mixing, boundary layer thickness, or wall-pressure fluctuations, there should be possibilities to implement this new theory in computational flow solvers.

Keywords: *Kinetic energy dissipation; onset and offset; wall surface roughness; defect web.*

1. Introduction

The knowledge of turbulence, as well as the transition into turbulence – in the relevant scientific literature – is stated to not be completely understood [1], [2], [3], [4].

The use of Navier-Stokes relations for the solving of viscous laminar flows works excellently, when applied to Newtonian fluids [5]. The default assumption within the sciences of turbulent flows is that the same set of relations valid for laminar flows is also valid for turbulent flows [1], [2].

In a parallel paper, a different perspective and approach to the problem of turbulent flows is presented: In short, the *slip flow process* is considered as a possible mechanism active in turbulent flows *at discrete locations*. By assuming a local generation of kinetic energy dissipation where slips occur, a candidate alternative fundamental model can be derived for turbulent flows [6].

A Maximum Entropy Production (MEP) process is assumed active, which generates- as well as influences the entire behaviour of a web of slips in a slowly evolving transient manner. For instance, the MEP process may result in a downstream "leakage" of slips [6].

Within a nominally "perfect" web fracture structure, "defect" zones can be assumed. These defect zones may downstream be "mended" from leaked slips (from an upstream position) – a process which may influence the overall apparent turbulent behaviour [6].

By assuming a connection between slip length L and slip flow velocity U_{slip}, as well as a spread-out of slips controlled by the slip resolution δ, it is possible to build a web of slips, in a way which approximately reproduces the experimentally known flow velocity profile of a pipe flow cross-section.

The specific selection of slip length and slip resolution is in these introductory computations not critical (perhaps these can be estimated at a later stage): This partly because a selection of a numerical value representing L automatically requires a specific numerical value representing δ for the correct time-averaged flow velocity profile to be met. Also, in case L is reduced by a factor of 50%, then δ is also reduced with a factor of 50%. The net effect is that since U_{slip} is reduced by 50% but occurs at two separated parallel positions instead of a single position, the net fluid flow representation will be approximately the same. However, the apparent kinetic energy dissipation rate per unit volume, assuming C_A would be independent of L, will reduce by 50%. But the latter is not the case: if the slip length L is reduced by 50%, then C_A is doubled, in order for the kinetic energy dissipation per unit volume in the split L and split δ situation to be the same as in the original L and original δ flake.

Hence, when discussing the fracture model, it is important to hold this in terms of a fully resolved turbulent boundary layer (in terms of L and δ), *i.e.* the viscous sub-layer, buffer layer, log-law region, and outer region, as well as the flow outside the turbulent wall boundary layer, must all be fully resolved zones in order to allow for a correct

*Corresponding Author

computation. Furthermore, the model coefficients C_A derived for a specific $L_{\max}$ should be represented in the form of the product $C_A L_{\max}$, where $L_{\max}$ is the assumed slip flow length within the viscous sublayer region, and C_A is the model coefficient for this selection of $L_{\max}$. In sum, regardless of the resolution of L and δ, the product $C_A L_{\max}$ will be numerically the same.

In order to obtain a correct time-averaged flow velocity profile, to be applied within the fracture structure, the traditional definition of a turbulent wall boundary layer is assumed, *cf.* Section 2. Also a preliminary accounting of the influence of wall surface roughness on the time-averaged flow profile is included in the analysis, *cf.* [6].

Section 2 presents a summary background on the scaling parameters used in the scientific field of single-phase turbulence to describe the turbulent wall boundary layer.

Also, an engineering example computation on turbulent air flow in a pipe section is presented, illustrating how different parameters can be computed, using a traditional engineering approach.

The same pipe geometry employed in this example is used also in Section 3, when testing the proposed model at different mean flow velocities and wall surface roughnesses. Beyond a discussion on initial results, the discussion also focuses on incorporating process thresholds and what type of errors and deviations can be expected from model-fitting a perfect web fracture structure to the experimental behaviour, when a model representation of a corresponding defect web fracture structure is not at hand.

Finally, the implications and consequences of a defect fracture structure is investigated in Section 4, where it is suggested that swirls may sometimes develop, followed by expansion, contraction or splitting.

2. Turbulent Boundary Layer

2.1 Traditional Definition

The extant literature assumes the following:

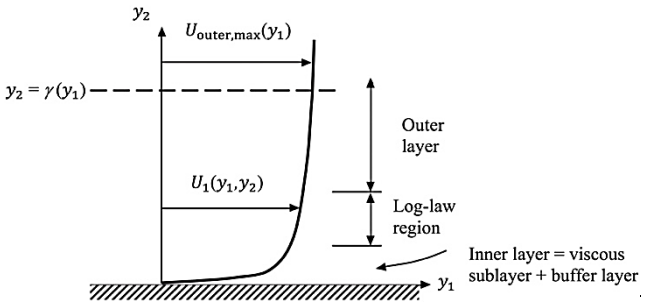

Figure 1. Typical time-averaged velocity distribution in a turbulent flow near a wall, according to [5]. (Not according to scale.) [Note: separate sources may have different definitions of the inner layer and outer layer, where sometimes the log-law region is included in both of these, and where the specific log-law region serves as an "overlap region".]

Assume τ_{wall} represents the wall shear stress, $U_{\text{outer,max}}$ the velocity at the edge of the outer layer, and $\gamma_{\text{outer,max}}$ represents and boundary layer thickness (defined by the y_2 position at the edge of the outer layer).

According to [5], it can be assumed that for the inner layer, the velocity U_1 is independent of the shear layer thickness (Prandtl proposition in 1930), *i.e.* $U_1 = b(\mu, \tau_{\text{wall}}, \rho, y_2)$, where μ is the dynamic viscosity and ρ is the density of the fluid. By dimensional analysis, this can be rephrased into the equivalent expression ${U_1}^+ = B({y_2}^+)$, which is referred to as the "law of the wall", where ${U_1}^+ = U_1/U^*$ and $U^* = (\tau_{\text{wall}}/\rho)^{1/2}$. Also, ${y_2}^+ = y_2 U^*/\nu$, where ν is the kinematic viscosity. The measure U^* is referred to as the "friction velocity" (as it is computed in the same units as velocity), although it does not represent any real flow velocity.

According to [5], it can be assumed that the velocity U_1 in the outer layer is independent of molecular viscosity but that its deviation from $U_{\text{outer,max}}$ depends on the turbulent flow layer thickness $\gamma_{\text{outer,max}}$ (Kármán 1933), *i.e.* $U_{\text{outer,max}} - U_1 = o(\gamma_{\text{outer,max}}, \tau_{\text{wall}}, \rho, y_2)$ in the outer layer. By dimensional analysis, this can be rephrased into the equivalent expression $(U_{\text{outer,max}} - U_1)/U^* = O(y_2/\gamma_{\text{outer,max}})$ in the outer layer, which is referred to as the "velocity-defect law" for the outer layer, where U^* represents the same friction velocity as for the inner layer.

According to [5], both the law of the wall, as well as the velocity-defect law, are found to be accurate for a wide variety of experimental situations in turbulent duct and turbulent boundary layer flows.

Furthermore, according to [5] these laws must overlap smoothly in the intermediary zone, which can only be the case if the velocity in the intermediary zone varies according to ${U_1}^+ = C^+ + \frac{1}{\kappa}\ln {y_2}^+$ (demonstrated by Millikan in 1937), hence reference of this zone as the low-law region. Here, the dimensionless constants $\kappa \approx 0.41$ and $C^+ \approx 5.0$.

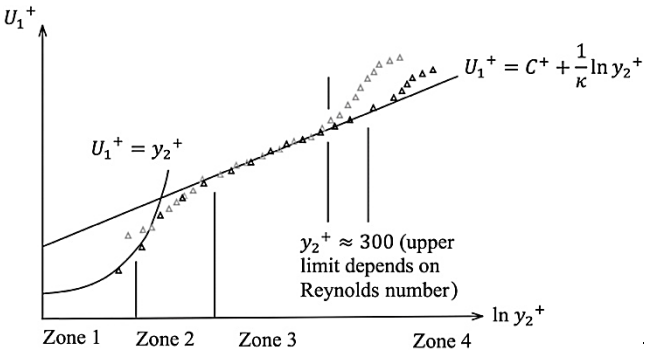

Figure 2. Time-averaged flow velocity in downstream wall direction, vs. distance from wall, across a turbulent wall boundary layer. White states that "Believe it or not, this figure, which is nothing more than a shrewd correlation of velocity profiles, is the basis for all existing "theory" of turbulent-shear flows." [5]

The following 4 zones are present inside the turbulent wall boundary layer:

Zone 1: The "viscous sublayer" – from the wall to approximately ${y_2}^+ \approx 8$.

Zone 2: The "buffer layer" – from approximately ${y_2}^+ \approx 8$ to ${y_2}^+ \approx 30$.

Zone 3: The "log-law region" – from approximately ${y_2}^+ \approx 30$ to ${y_2}^+ \approx 300 - 1000$.

Zone 4: The outer region – typically represents 80% of total thickness of turbulent wall layer.

An exterior zone, identified as the flow outside the turbulent wall boundary layer, can be attributed to as a fifth zone:

Zone 5: outside the outer layer, *i.e.* outside the turbulent wall boundary layer.

Table 1: Computations. The net integrated kinetic energy dissipation across a 1 m pipe, across the radius, using Eq. (18) in [6]*, for below flow cases, arrives at a number multiplied by $C_A L_{\max}$. This number is compared to the corresponding experiments computed using Eq. (13) in* [6]*. The $C_A L_{\max}$ coefficient is determined resulting in the net kinetic energy dissipation of the computations matching the corresponding experiments. Time-averaged mass flow rates in full agreement. Time-averaged velocity profile is in full agreement.*

Re	f	τ_{wall} (N m^{-2})	ε/D	U_{mean} (m s^{-1})	$C_A L_{\max}$ (m^2 s^{-2})	% of $\frac{\mathrm{d(KE)}}{\mathrm{d}t}$ in v. subl.	% of $\frac{\mathrm{d(KE)}}{\mathrm{d}t}$ in buffer r.	% of $\frac{\mathrm{d(KE)}}{\mathrm{d}t}$ in log-law
5000	0.03739	0.001638	0	0.5393	0.002103	60.0	36.1	3.9
5000	0.03745	0.001641	0.00005	0.5393	0.002105	60.0	36.1	3.9
5000	0.03795	0.001663	0.0005	0.5393	0.002114	59.8	36.2	3.9
5000	0.04261	0.001867	0.005	0.5393	0.002178	58.2	37.9	3.9
5000	0.07595	0.003327	0.05	0.5393	0.002695	82.8	17.2	0.0
10000	0.03088	0.005415	0	1.079	0.007380	58.2	35.9	5.9
10000	0.03096	0.005429	0.00005	1.079	0.007386	58.2	35.9	5.9
10000	0.03164	0.005549	0.0005	1.079	0.007445	58.0	36.0	6.0
10000	0.03763	0.006599	0.005	1.079	0.008109	58.0	38.8	3.2
10000	0.07380	0.01294	0.05	1.079	0.01052	82.6	17.4	0.0
100000	0.01799	0.3155	0	10.79	0.5251	54.6	34.5	8.5
100000	0.01826	0.3202	0.00005	10.79	0.5290	54.6	34.5	8.5
100000	0.02033	0.3565	0.0005	10.79	0.5587	54.7	34.8	8.4
100000	0.03131	0.5491	0.005	10.79	0.7179	56.6	38.6	4.8
100000	0.07178	1.259	0.05	10.79	1.028	82.4	17.6	0.0
1000000	0.01165	20.43	0	107.9	41.39	53.6	33.9	8.7
1000000	0.01265	22.18	0.00005	107.9	43.14	53.6	34.0	8.7
1000000	0.01721	30.18	0.0005	107.9	50.66	54.0	34.4	8.7
1000000	0.03047	53.43	0.005	107.9	71.14	56.9	38.9	4.2
1000000	0.07157	125.5	0.05	107.9	102.5	82.4	17.6	0.0

2.2 Example (Traditional Engineering Approach)

The discussion centres around Example 6.3 in [5]: Air at 20 ˚C flows through a 14-cm-diameter tube under "fully developed" conditions. The centreline time-averaged velocity is $U_{\max} = 5$ m/s. The following computation demonstrates how Fig. 2 can be used to compute (a) the friction velocity U^*, (b) the wall shear stress τ_{wall}, and (c) the average velocity U_{mean}.

In order to compute (a), White [5] argues that the log-law relation can be assumed accurate to the centre of the tube, *i.e.* at the centre: $U_1 = U_{\max}$, $y_2 = R$ and the log-law relation can be expressed as: $\frac{U_{\max}}{U^*} = 5.0 + \frac{1}{0.41}\ln\frac{RU^*}{\nu}$. Since $U_{\max} = 5$ m/s and $R = 0.07$ m, the friction velocity U^* is the only unknown parameter. The solution can be estimated – by trial and error – $U^* = 0.228$ m/s, according to [5], where the kinematic viscosity of air is $\nu = 1.51 \times 10^{-5}$ m^2/s from literature tables.

In order to compute (b), assuming a normal atmospheric pressure of 1 atm, gives $\rho = 1.205$ kg/m^3. Since $U^* = (\tau_{\text{wall}}/\rho)^{1/2} = 0.228$ m/s, the wall shear stress can be directly computed as $\tau_{\text{wall}} = 0.062$ Pa.

In order to compute (c), the average velocity U_{mean} can be found by integration of the log-law relation: $U_{\text{mean}} = \frac{1}{\pi R^2}\int_0^R U_1 2\pi r\,\mathrm{d}r$, *cf.* [5]. Introducing $U_1 = U^*\left[C^+ + \frac{1}{\kappa}\ln\left(\frac{y_2 U^*}{\nu}\right)\right]$, and substituting y_2 with $R - r$, the integration can be performed. The computed result is: $U_{\text{mean}} = 0.835 U_{\max} = 4.17$ m/s.

Finally, it is good to verify that the flow is really turbulent, which can be done by checking the Reynolds number $\mathrm{Re} = U_{\text{mean}} D/\nu = 38700$. Here it is greater than 4000[1], and hence the flow is clearly turbulent [5].

Note that several results can be obtained from the velocity correlation, without need of solving any basic relations.

Finally, it is interesting to compare the shear stress of the wall in case a hypothetical laminar flow of air at would be present in the same tube, with the same average flow speed of air $U_{\text{mean}} = 4.17$ m/s: From the text following Eq. (12) in [6] the shear stress at the wall for laminar flows was computed as $\tau_{\text{wall,laminar}} = 2\mu U_{\max}/R =$ [*cf.* Eq. (4) in [6]] $= 4\mu U_{\text{mean}}/R = 0.0043$ Pa, *i.e.* approximately 7% of the wall shear stress for the laminar flow situation as compared to the turbulent flow situation.

[1] The ranges of Reynolds numbers where the flow is considered to be laminar, "transitional", or turbulent depend on to what degree the flow is disturbed: In fact, vibrations of the pipe, surface roughness of inner walls (entrance region) may trigger turbulent flows to occur at lower Reynolds numbers. Furthermore, artificial disturbances, such as adding a so-called "trip wire" (which is common in turbulent laboratory experimental setups) or subjecting the pipe to a sound-shock wave, may trigger turbulent flow behavior at even lower Reynolds numbers. However, for many engineering applications the flow in a pipe can be assumed to be laminar if the relevant Reynolds number is less than approximately 2100, and turbulent if the Reynolds number is greater than approximately 4000. Between these numbers, the flow may switch between laminar and turbulent in an apparently random manner, which in the field of fluid dynamics is referred to as a transitional flow condition.

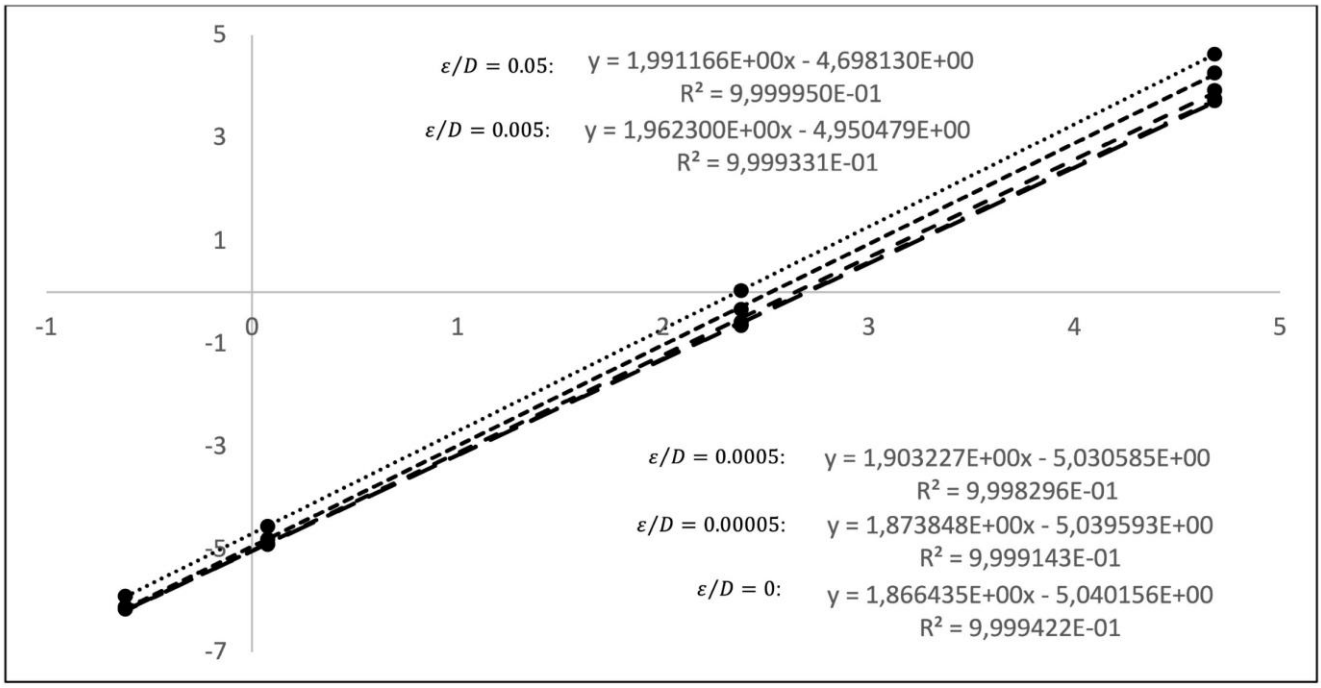

Figure 3: The x-axis is here represented by $\ln(U_{\text{mean}})$*, and the y-axis is represented by* $\ln(C_A L_{\max})$.

3. Applying the Proposed Model

3.1 Computations – 20 Cases

Computations are made for the same geometry, fluid and temperature as described in Section 2.2, however at different velocities U_{mean} and different relative surface roughness ε/D, listed in Table 1 for 20 cases, together with the corresponding results. These 20 cases were selected to cover a wide range of pipe flows at subcritical velocities ($M < 1/3$). All computations assume a 1-metre-long pipe section, and where the resulting $C_A L_{\max}$ value represents the value which gives 1st law agreement between experiment and the corresponding perfect fracture model computation. The Darcy friction factor f is computed from the Colebrook equation (providing 1-2% accuracy in determining f for the entire Moody diagram). The non-dimensional velocity variations ${U_1}^{++}$ *vs.* ${y_2}^{++}$ following the Section 2.7 and Fig. 8 in [6] are assumed, where C^{++} varies between 5.0 and 7.0 depending on surface roughness. Also, $L/L_{\max}$ following Fig. 9 in [6] is assumed, *i.e.* the variation in $L/L_{\max}$ *vs.* ${y_2}^{++}$ depends on the surface roughness.

3.2 Graphical Presentation of Results

A number of statements, as well as interpretations, can now be made, looking at these results and comparing them with a Moody diagram.

First: Since the trends are rather clear in terms of mean velocity as well as relative surface roughness, interpolation can be used to estimate the $C_A L_{\max}$ value, *cf.* Fig. 3. Using the proposed fracture model, and integrating radially as well as axially, the local kinetic energy dissipation (per unit volume), will result in a net kinetic energy dissipation rate approximately equal to the estimations obtained with the Colebrook equation and Eq. (13) in [6].

Second: The correlations presented in Fig. 3 appear to reflect a connection between $C_A L_{\max}$ and approximately – but not exactly – the square of the mean velocity:

For relative roughness $\varepsilon/D = 0.05$:

$$C_A L_{\max} = e^{-4.698130} (U_{\text{mean}})^{1.991166} \quad (1)$$

(for $5000 < \text{Re} < 1000000$)

For relative roughness $\varepsilon/D = 0.00$:

$$C_A L_{\max} = e^{-5.040156} (U_{\text{mean}})^{1.866435} \quad (2)$$

(for $5000 < \text{Re} < 1000000$)

Third: The correlation presented in Fig. 4 indicate that while $C_A L_{\max}$ shows a strong variation depending on Reynolds number, it appears that $C_A L_{\max}$ varies moderately when changing the surface roughness (at a fixed Reynolds number). For instance, at $\text{Re} = 5000$, the difference between $C_A L_{\max}$ at relative roughness $\varepsilon/D = 0.05$ and $C_A L_{\max}$ at relative roughness $\varepsilon/D = 0.00$ is only a factor 1.28, and at $\text{Re} = 1000000$, the difference between $C_A L_{\max}$ at relative roughness $\varepsilon/D = 0.05$ and $C_A L_{\max}$ at relative roughness $\varepsilon/D = 0.00$ is only a factor 2.48. This relatively small variation is interesting at low Reynolds numbers, in the context of $C_A L_{\max}$ as a proposed critical parameter for the transition at certain Re numbers, both in the nominal model (*cf.* Section 2.9 in [6]) and for the more advanced model (*cf.* Section 3.3). A limited variation in $C_A L_{\max}$, at low Reynolds numbers, suggests a similar range in Re numbers, where transition from laminar flow to an onset of the turbulence process can occur, regardless of surface roughness.

3.3 Onset and offset of turbulence

Consider the Re numbers at which turbulence is onset, *i.e.* the mean flow velocity, if starting from a flow rate at laminar flow conditions, which is steadily increased – until turbulence onset is triggered. The typical onset condition for turbulence in pipe flows, is stated to occur at Re numbers around 2300.

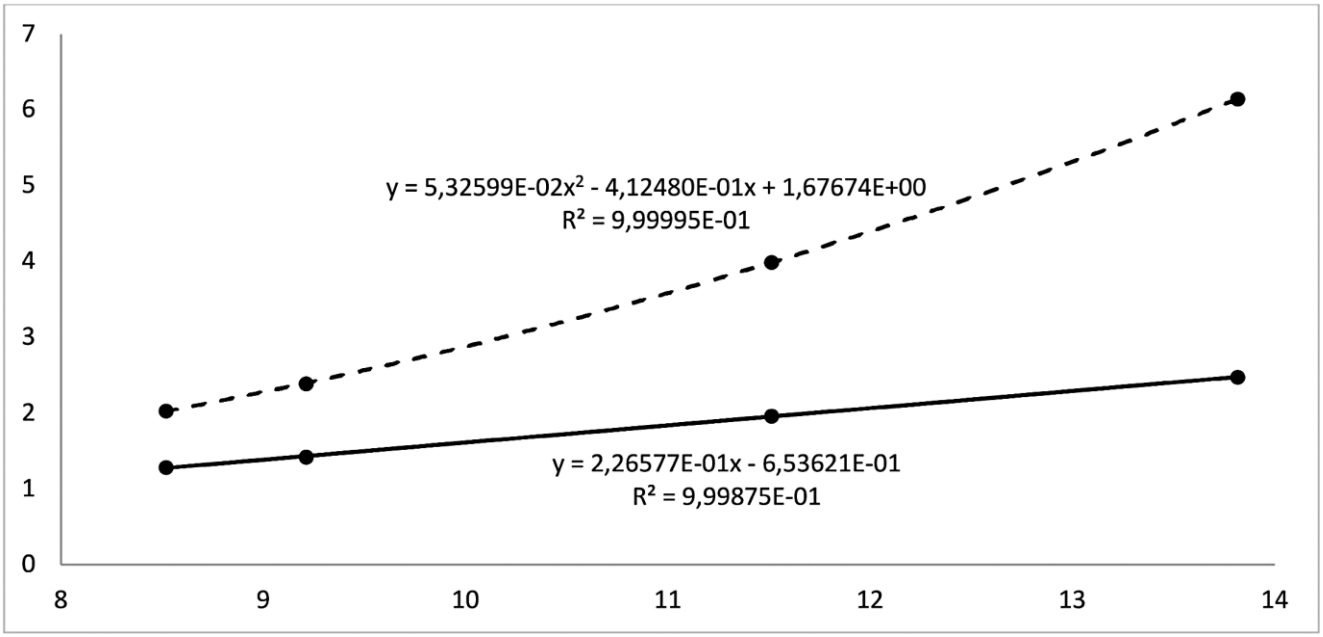

Figure 4: The x-axis represents ln(Re). *The full line represents the ratio* $\{C_A L_{\max}(\varepsilon/D = 0.05)\}/\{C_A L_{\max}(\varepsilon/D = 0)\}$ – *which appears to vary linearly with* ln(Re), *for the present computations. The hashed curve represents the ratio* $\left\{\frac{\mathrm{d}(KE)}{\mathrm{d}t}(\varepsilon/D = 0.05)\right\}/\left\{\frac{\mathrm{d}(KE)}{\mathrm{d}t}(\varepsilon/D = 0)\right\}$ – *which varies against* $\ln(\mathrm{Re})$ *following a polynomial expression.*

It turns out that the Re number at which turbulence offsets (or disappears) will be different, if running this experiment in the opposite direction, *i.e.* starting from a turbulent flow condition, and steadily decreasing the flow rate until a transition occurs (to laminar flows).

The estimation in Eq. (23a) in [6] predicts a transition Re number around 870 for $\varepsilon/D = 0$ in the case depicted in Fig. 3 (or by using Eq. (2)) – where we note that we have assumed the same relation for extrapolation outside the valid range $5000 < \mathrm{Re} < 1000000$.

The alternative estimation in Eq. (23b) in [6] predicts a transition Re number around 975 for $\varepsilon/D = 0$ in the case depicted in Fig. 3 (or by using Eq. (2)). Also in this case, the variation of f *vs.* Re number, and variation of $C_A L_{\max}$ required extrapolations outside the valid range.

Hence, both these nominal estimations project the onset of turbulence to occur around 2.5 times lower than the experimentally obtained Re number for turbulence onset. Possibly, utilizing these two relations would however – possibly – be a good indicator for the offset Re number of turbulence.

In order to approach this apparent deviation in turbulence onset, we turn to experimental observations:

The literature provides an excellent range of descriptions on the various forms of instabilities and flow behaviours prior to the onset of the turbulence, *cf. e.g.* [1].

One of the final forms of structures that appears just prior to the onset of a turbulent wall boundary layer, a structure that the relevant literature has focused on significantly *cf. e.g.* [1], [7], [8], [9], [10], [11], is the so-called turbulent spot. Arguably, the flow appears to be laminar on one side of the spot, while turbulent on the other side. Considerable experimental work on studying turbulent spots has been made, and the reason for stating the arrowhead forward side as representing a turbulent flow is that the identical mean flow velocity variations *vs.* distance from the wall is observed inside the turbulent side of the turbulent spot, as compared to the regular variations found in a fully-developed turbulent wall boundary layer.

True, the turbulent spots behave in a strange way, as they first occur as spots – which grow in-plane in both y_1- and y_3-directions (for a flow in the y_1 direction, and where y_2 axis represents the normal direction from the wall plane spanned by the y_1-axis and y_3-axis unit vectors, *cf.* Fig. 1) when following their formation. Due to activities occurring inside a spot, the spot will span about the **total thickness** of a turbulent wall boundary layer (*i.e.* the thickness of inner + outer layers). In a pipe flow, the front arrow-head forward side of the turbulent spot will move at about 2/3 speed of U_{mean}, while the rear laminar side of the turbulent spot will move around 1/3 the speed of U_{mean}.

There are experimental observations made on the presence of "hairpin-" or "horse-shoe" vortexes on the turbulent side, near the wall, which **perhaps form an experimental indicator** of the influence the discrete web-slip structures with separated δ.

Although the real flow in a turbulent spot involves flows in all three dimensions y_1-, y_2- and y_3 (a necessity according to the equation of continuity), and while the nominal transition model **only** accounts for irreversible thermodynamic processes occurring in the y_1-direction, one might contemplate the possibilities of irreversibilities in primarily the y_2-direction (as well as some effects in the y_3-direction flow). However, the author of the present work does not believe this to be the case.

Also, looking at the theory, there appears to be no clear candidate regarding the residual thermodynamic *no process* behaviour that would provide the possible threshold behaviour – *cf.*, *e.g.* similar reasoning on the difficulties on finding a threshold behaviour for Coulomb friction (*cf.* [12]).

However, one observation that is made experimentally, considering particle trajectories when inserting small particles into and around a turbulent spot, is that the turbulent spot appears to exhibit some "suction" process of fluid flow on the laminar side.

Considering the assumed conditions 1-4 in Section 2.9 in [6], and the presence of turbulent spots – which scientists

have focused on regarding the onset of turbulence, the conditions 1-4 may need to be slightly reconsidered:

Condition 1: Assuming the transition occurs in a turbulent spot, this is strictly speaking a rather spread-out zone. Hence, in order to improve the nominal model for turbulence onset, one may need to consider conditions for the laminar *vs.* turbulent **transformation to occur at slightly different positions**.

Condition 2: Assuming equal kinetic energy dissipation conditions is probably reasonable. However, the turbulent spot itself alters the flow velocity and thus the local kinetic energy dissipation, which is relevant for this transition formula to work well. Hence, the overall U_{mean} velocity gradient cannot be used to directly compute the wall viscous dissipation – assuming no velocity interruption on the laminar flow side. Hence, it is assumed that **the laminar flow velocity gradient for the kinetic energy dissipation needs to be adjusted**.

Condition 3: Not applicable, if reconsidering the positions of transformation to occur (Condition 1).

Condition 4: Still valid. The process transition is still believed to occur in the vicinity of a solid wall.

Considering the particle trajectories in the experimental observations in Fig. 7 on p. 134 in [9], and also the experimental observations to the effect that the same turbulent flow wall behaviour is observed on the turbulent side of the turbulent spot, the computations can be adjusted according to the following: the viscous laminar kinetic energy dissipation on the laminar side can assume a – say – **50% higher laminar flow velocity gradient** (as compared to the nominal velocity gradient value), while the kinetic energy dissipation – and local flow gradient - for the turbulent side is extracted without any alternations as compared to the nominal computations in [6].

This gives for the viscous laminar side:

$$\frac{\mathrm{d(ke)_{viscous}}}{\mathrm{d}t} = \mu\left(\frac{1.5\partial U_1}{\partial y_2}\right)^2 \tag{3}$$

where $\partial U_1/\partial y_2$ is computed for the laminar flow not assuming the presence of a turbulent spot.

On the turbulent side, the kinetic energy dissipation is:

$$\frac{\mathrm{d(ke)_{res}}}{\mathrm{d}t} = C_A\frac{\rho L}{\delta}U_{\text{slip}} \approx C_A\rho L_{\max}\frac{\partial U_1}{\partial y_2} \tag{4}$$

cf. Eq. (21) in [6].

Hence, equating Eq. (3) with Eq. (4) at the onset transition point, gives:

$$2.25\mu\left(\frac{\partial U_1}{\partial y_2}\right)^2 - C_A\rho L_{\max}\left(\frac{\partial U_1}{\partial y_2}\right) = 0 \tag{5}$$

Which gives a revised formula for the onset transition point according to:

$$\frac{18{U_{\text{mean}}}^2}{C_A L_{\max}} = \frac{\rho U_{\text{mean}} D}{\mu} = \text{Re} \tag{6}$$

For a perfectly smooth pipe wall surface with $\varepsilon/D = 0.00$, we can insert Eq. (2) in Eq. (6), which gives onset at Re=2310 for the case depicted in Fig. 3.

Note: To be clear, the author did not select "50% higher laminar flow velocity" from any data source, other than identifying a likely larger inflow velocity gradient on the laminar side of the turbulent spot compared to the situation if the turbulent spot would not be present. The specific selection of 50% higher inflow velocity was intentionally selected in order to arrive at a matching turbulent onset Re number, as found in experiments. In any case, Eq. (6) is a **proposed improved model for the onset of turbulence**, where the influence from wall surface roughness can be accounted for.

Experimentally, if a tracing fluid is injected into a core of a pipe, one may find that the turbulence onset is associated with an apparent "burst", "flash" or "puff" which might trigger near (but just below) the transition Reynolds number. An interpretation of this suggests the quick and immediate development of a local fracture structure around and near the wall transition point. If there for some reason would not be enough kinetic energy available to maintain this onset structure the burst will quickly die out, and the flow will return to the viscous laminar flow situation.

Interestingly, the presence of "bursts" appears also to exist after turbulence boundary layer onset, *cf. e.g.* [13], which might suggest the sudden and local development of ordered web fractures within a geometric region of large defects (after turbulence onset). An interesting finding by [13] was that the intermittency of these boundary-layer bursts appears to connect with "outer" variables – which if one would allow oneself to speculate might further suggest a direct connection with the consumption of kinetic energy from the overall surroundings.

Regarding the matter of **turbulence offset**, note that there is no corresponding Re number, lower than the nominally proposed transition Re number in Eqs (23a-3) in [6], since there is no experimental evidence on the formation of turbulent spots when reducing the average velocity of a turbulent flow.

Consider the situation when the flow is reduced, and the available kinetic energy to be dissipated is reduced below a critical point: In such case, the web-fracture flow will release from the wall surface, flow downstream, and eventually die out (similarly as described in Section 2 in [6]). The flow that replaces the web structure at the original position is a viscous laminar flow.

3.4 Defect *vs.* Perfect Web-Fracture Structure

First, consider a model-fitting of a perfect web fracture structure to an experiment, which gives a net kinetic energy dissipation. This is followed by estimating the volume of defect zones, while assuming these defect zones to be suddenly present in this model-fitted perfect web structure. For this artificially-assumed defect web fracture structure, the net kinetic energy dissipation is estimated. What is the difference in net kinetic energy dissipation between these two cases?

Second, consider a model-fitting of a defect web fracture structure to an experiment – assuming a certain distribution of defect zones. How much would the model-fitted parameter $C_A L_{\max}$ for the defect web fracture structure differ from the model-fitted parameter $C_A L_{\max}$ if assuming a perfect web structure?

Start with estimating the first difference of interest:

Consider the locations of the defects: None would occur in the viscous sublayer region, as this is concluded experimentally: recall that "nothing happens in the viscous sublayer region" according to scientists.

Most would occur in the buffer layer, due to the presence of non-symmetry in both L and δ, followed by the log-law region (only non-symmetric in terms of δ).

The presence of a local defect means that the defect zone does not represent a zero kinetic energy dissipation, but perhaps a reduction of X% (per unit volume) compared to the corresponding perfect web fracture structure.

The volume occupied by a defect zone is difficult to estimate (due to a lack of experimental data), and it is noteworthy that not all defect zones would necessarily result in the generation of swirls or offset eddies. However, defect zones always reduce the kinetic energy dissipation rate (per unit volume).

The downstream effects of a generated swirl are a complicating factor, as discussed in Section 4: The generated swirl may offset downstream behaviour which may appear to displace locally the δ and L. However, as argued in Section 4, it would seem unrealistic that the large visible offsets in L and δ – which give large downstream fluctuations – result in very different net kinetic energy dissipations in the large-scale offset defect structures, as compared to the nominal non-offset perfect web fracture structures. The defect web fracture structure condition should be considered a thermodynamically rather stable condition, as the generation of a local defect does not trigger multiple downstream defects. The latter would locally trigger separate eddies, literally resulting in an uncontrolled explosion of events (a true thermodynamic instability condition). No: from a single defect zone, a long eddy may be generated, and it is assumed that the point of origination can be identified – also when the defect zone is flowing downstream.) Hence, it is assumed that the most important view (for net kinetic energy dissipation computations) is to solely focus on the nominal defect zones as locally-distributes zones or clouds within the turbulent flow.

Example 1: Re $= 5000$, and $\varepsilon/D = 0$ for flow condition described in Table 1.

Assume that 15% of the buffer region contains defect zones, and 15% of the log-law region. (Of the 15% of the buffer region perhaps only 3% generates swirls, and of the 15% in the log-law region, perhaps only 2% generates swirls.) Assuming furthermore that the defect zones reduce the kinetic energy dissipation by 50% (a crude guess with no experimental support), the net effect on the total net kinetic energy dissipation can be estimated as:

Viscous sublayer: 60.0% of nominal net kinetic energy dissipation = no effect

Buffer layer: 36.1% of nominal net kinetic energy dissipation → reduction to: 85%*100% + 15%*50%=92.5% of nominal → reduction to 36.1%*0.925 = 33.4%

Log-law region: 3.9% of nominal net kinetic energy dissipation → reduction to: 85%*100% + 15%*50%=92.5% of nominal → reduction to 3.9%*0.925=3.6%

Hence: A reduction in net kinetic energy dissipation = approximately equal to difference in net kinetic energy dissipation between defect web fracture and perfect web fracture: from 100% to 60.0%+33.4%+3.6%=97.0%, *i.e.* a **difference of around 3%.**

Example 2: Re $= 1000000$, and $\varepsilon/D = 0.05$ for flow condition described in Table 1:

Assume that 15% of the buffer layer contains defect zones (of the 15% of the buffer layers perhaps only 3% generate swirls, and of the 15% in the log-law region, perhaps only 2% generate swirls.) The log-law region does not seem to pertain for this flow case, as there are no time-average flow gradients in the core zone from the centreline position in the pipe, all the way to the buffer region. Assuming that the defect zones reduce the kinetic energy dissipation by 50% (a crude guess with no experimental support), the net effect on the total net kinetic energy dissipation can be estimated as:

Viscous sublayer: 82.4% of nominal net kinetic energy dissipation = no effect

Buffer layer: 17.6% of nominal net kinetic energy dissipation → reduction to: 85%*100% + 15%*50%=92.5% of nominal → reduction to 17.6%*0.925 = 16.3%.

Hence: A reduction in net kinetic energy dissipation = approximately equal to difference in net kinetic energy dissipation between defect web fracture and perfect web fracture: from 100% to 82.4%+16.3%=98.7%, *i.e.* a **difference of around 1%.**

Regarding the second difference of interest, a model fitting of a hypothetically defect fracture structure to turbulence pipe experiments would arrive at precisely the same wall shear stresses as fitted for the perfect web fracture structure (*i.e.* the same 1st law balance agreement between experiment and corresponding defect fracture computation can be obtained); yet the difference in the resulting $C_A L_{\max}$ for these two cases – perfect web *vs.* defect web – is likely rather small (likely within the 1-3% range).

3.5 Defect Web-Fracture Structure on General Trends

Consider the computed trends in Fig. 3. Is there anything suggesting that these trends may connect, somehow, with any defect web fracture structure?

A partial answer may be obtained by reformulating this question: Explain the variations of $C_A L_{\max}$ proportional to ${U_{\text{mean}}}^{1.87}$ to ${U_{\text{mean}}}^{1.99}$, and also explain what would it take utilize the proposed model to reach a theoretical variation of $C_A L_{\max}$ proportional to ${U_{\text{mean}}}^{2}$?

Considering the proposed fundamental model, it appears that for high Re numbers, and also for high ε/D numbers, the variation of $C_A L_{\max}$ approaches being proportional to ${U_{\text{mean}}}^{2}$, however, it does not fully reach this variation.

Considering the fundamental model:

$$\frac{\mathrm{d(ke)_{res}}}{\mathrm{d}t} = C_A \frac{\rho L}{\delta} U_{\text{slip}} \tag{7}$$

and hypothetically assume that only the viscous sublayer dissipates kinetic energy. As the viscous sublayer zone is very close to the wall (and relatively thin in terms of the entire pipe diameter, although rather thick in terms of ${y_2}^{++}$ number), this would resemble a situation similar to that of a solid plug which moves at velocity U_{mean} and with a $C_A L_{\max}$ that correlates with ${U_{\text{mean}}}^{2}$.

Hence, it appears that it is not the defect fracture structure that hinders $C_A L_{\max}$ from being proportional to ${U_{\text{mean}}}^{2}$. Instead, it seems that the distribution of kinetic energy dissipation across the pipe has variations mostly due to variations in velocity at different pipe radii – preventing all kinetic energy dissipation from occurring near the solid wall.

In sum, it appears that defects in the fracture structure would not have any major influence on the trends in Fig. 3.

3.6 Scaling Laws in Context of Proposed Model

It is not immediately obvious whether dimensional analysis applies to situations involving discrete relations. Apparently, some kind of linear relationship may be required with intersection at 0 in order to allow for a dimensional analysis. On this matter, note that the approximations of assumed connection between slip velocity and slip length, *cf.*

Eq. (14) in [6], as well as the assumption $\tau \propto U_{\text{slip}}$ in [6], both represent linear relationships with intersection at 0.

Even though possible offsets from linearity, as well as offsets from intersections at 0, may occur for defect web fractures, it is reasonable to assume that such offsets would not occur for the saturated flakes in the viscous sublayer.

In most of computations in Table 1, the kinetic energy dissipation in the outer layer is 0, or comparatively negligible. For a couple of computations, the kinetic energy dissipation in the outer layer accounts to a maximum around 4% of the total kinetic energy dissipation.

In the derivation of the "velocity-defect law" for the outer layer by dimensional analysis, described in Section 2.1, it is assumed that the mean velocity U_1 is independent of molecular viscosity. This statement is arguably similar to assuming that no viscous dissipation is occurring in the outer layer, or more generally, that no kinetic energy dissipation is occurring in the outer layer. This is in line with present theory and present computations. Hence, the traditional scaling correlations proposed in Section 2.1 for the outer region should arguably also apply for present computations.

On the matter of inner-layer velocity, if molecular viscosity does not play a role in the velocity variation in the viscous sublayer – according to the proposed new theory – arguably one should be able to make similar assumptions regarding the scaling of the viscous sublayer as for the outer region:

$$U_1 = o_{\text{vs}}\left(\gamma_{\text{viscous sublayer, max}}, \tau_{\text{wall}}, \rho, y_2\right) \tag{8}$$

allows for the derivation of the expression ${U_1}^+ = C_{\text{vs}} {y_2}^+$, where we have utilized the observation from the viscous sublayer that $L = L_{\max}$ and $\delta = \delta_{\min}$ are equal for neighbouring flakes in the y_2-direction.

For the buffer layer, a corresponding scaling as for the outer region is called for:

$$U_1 = o_{\text{bl}}\left(\gamma_{\text{buffer layer, max}}, \tau_{\text{wall}}, \rho, y_2\right). \tag{9}$$

This gives:

$${U_1}^+ = O_{\text{bl}}\left({y_2}^+ / {y_2}^+_{\text{buffer layer, max}}\right) = O_{\text{bl},2}({y_2}^+) = B({y_2}^+), \tag{10}$$

i.e. an identical "law of the wall" is obtained for the buffer layer, but derived from a different perspective, and utilizing different original assumptions.

In sum, the same scaling parameters as the original ones employed in the traditional theories dating back to the 1930's can be employed with present theories.

The traditional theory assumption $C_{\text{vs}} = 1$ for the viscous sublayer come from the traditional fundamental model assumption between shear stress and strain rate, *cf.* Section 5, and is hence not connected with any scaling law.

The present theory opens up the possibility that $C_{\text{vs}} \neq 1$. In fact, one would expect a different value from 1, in the context of present theory. (Possibly, if δ resolution can be observed in the viscous sublayer, the velocity profile may appear to be similar to a "stair-case" variation with y_2.)

Note: The computations in Table 1 all assume $C_{\text{vs}} = 1$ in the viscous sublayer for the computation of the velocity variation with y_2. There is at present no suggestion of a better value to use. Even with a different coefficient value, equally-good and equally-stable general correlations as obtained in computations in Section 3.1 can be assumed.

4. Generation of Swirls with Proposed Model

The numerical simulation of swirls and eddies has proven difficult when employing traditional turbulence theory. It appears difficult to find any significantly increased kinetic energy dissipation in these simulation results. The inability to find the levels of kinetic energy dissipation (or viscous dissipation) anywhere close to the levels observed in experiments is a major problem.

The new theory here proposed completely alters the need for studying the generation of swirls and eddies: For the purpose of finding out where the overall kinetic energy dissipation occurs in a turbulent wall boundary layer, the results with the present theory have provided clear answers – swirls and eddies appear to have negligible to no impact on the overall kinetic energy dissipation.

However, there may be a remaining interest in numerically simulating swirls and eddies – for instance for the study of pressure fluctuations at walls as caused by turbulence.

The following aspects may influence the generation of swirls for the new proposed model:

- Local and instantaneous conditions such as: (a) large imbalances of forces that may occur at defect zones.
- Wide, transverse span-wise processes across a wall influencing the MEP processes, or as a result of the MEP processes, such as: (b) local deficiency in kinetic energy at hand for dissipation, during redistribution, resulting in defect zones appearing. (c) following the principles of far-from-equilibrium ("order by fluctuations" principle), the downstream movement of defect zones (these can be visualized as *clouds*) may occur in a cyclical manner, *i.e.* clouds of defects generated upstream in a repeat manner (at a certain frequency), which moves downstream. In this way, long-downstream-, or large transverse span-wise coherent structures may be generated.
- History or memory effects: (d) Connecting with (c) is the proposed new theory's downstream movement of slips (the R.Th.D.p. zones) – and possibly additional leakage phenomena. A connection can be made to an earlier "history theory" described in [14]. This history theory assumes that:

  "the turbulence which produces the shear at any point has its origin at the surface upstream from its present location".

  Ross and Robertson's history theory was arguably designed to be applied for airfoils and diffusers where the following general assumption does not hold [14]:

  "For the case of flow with zero or small pressure gradients, the flow conditions and the wall shear stress do not vary significantly in the direction of flow, and one can correlate the entire boundary layer distribution with local conditions."

  In agreement with this latter statement, all computations in this paper assumed local conditions at a pipe intersection. However, the author of this paper yet believes such history and memory effects are possible to observe experimentally. Partly, the downstream movement of the slips (or R.Th.D.p. zones) will generate

apparent eddies which appear to be stretched in the direction of the fluid flow, which in turn connects with experiments on the anisotropy level of turbulence: Experiments indicate a much larger degree of observed turbulence anisotropy, as compared to the corresponding simulations, which tend to display more isotropic turbulence when modelling according to the traditional approach. Furthermore, the accumulated effect of downstream leakage will for very long (smoothly polished) narrow pipes eventually lead to turbulence to apparently disappear, *i.e.* overall turbulence behaves in a slowly evolving transient manner in agreement with experimental observations [17], [18], [19].

In this context, it is interesting to re-cite Ross and Robertson's [14] recounting of the space-history theory proposed by Schultz-Grunow [15] based on the original experiments by Jacobs [16]:

"Jacobs measured the change in the velocity profile along a smooth surface preceded by a rough surface. An analysis of these profiles yielded the shear stress distribution at several stations. As shown in Fig. 1 (in [14]), Jacobs found that the shear stress gradient in the outer portion of the boundary layer retained the value which it had had over the rough surface for a considerable distance along the smooth surface, while the wall shear fell almost immediately to its smoothest-surface value. Jacobs also studied the flow from a smooth to a rough surface, and he again found that the upstream shear stress gradient persisted for a considerable distance, the rough-surface shear gradually being diffused across the boundary layer as the flow proceeded downstream. As noted by Schultz-Grunow, these experiments clearly establish the importance of the history of the flow."

Connected with the generation of swirls is the phenomenon of eddy growth, which here is assumed to connect with these points. In particular, the author believes that the history- or memory effects may contribute considerably to the growth of eddies.

5. Discussion

The traditional theory has issues to resolve which are partly summarized in Table 1 in [6]. In the review paper by George [4], these issues are further discussed.

George states that (A) "Over the past decade **almost every aspect of our traditional beliefs about wall-bounded flows has been challenged**." Furthermore, George states that "No matter whether we pay our allegiance to the traditional ideas or the new ones, **the continuing difficulties** with computations of complex wall-bounded flows (or even simple flows with pressure gradients) **suggest strongly that we have missed something important**." [4]

Considering the gradual improvements in experiments, and supporting CFD computations, George furthermore states that (B): "So confident was the turbulence community in its beliefs that **virtually no one even bothered to measure the skin friction**, and it was simply inferred from fitting the log profile to a few points near the wall, usually for values of y+ between 30 and 100. In fact the 'log'-based ideas were so well-accepted that it seemed to bother only a few that **real shear stress measurements** (both momentum integral and direct) **differed consistently and repeatably from these inferred results**." [4]

On the matter of options to take to resolve the issues, George states that (C): "**Instead of causing a re-examination of the theory**, it became common wisdom that there was something wrong with these techniques. The careful drag and mean velocity measurements laboriously performed in the 30's and 40's were discarded as being in error." [4]

In contrast, *the present work focuses on re-examining the theory utilizing a fundamentally different discrete process*, which allows for the time-averaged velocity profile to be accurately reproduced, and in addition allows for the 1st law balance of the simulations to match the corresponding 1st law balance of the experiments – for several different pipe flows.

It should be noted that many experimental tools are designed assuming the Navier-Stokes relations for laminar flows to be valid. Caution on which reference experiments to select in the present case is warranted.

The very "careful … mean velocity measurements laboriously performed in the 1930's and 1940's", are the basis of the computations in this paper, as this reference data represents experimental data obtained using experimental tools **not requiring the validity of the viscous laminar flow correlation between shear stress and strain rate**.

Although some experiments appear questionable, the author recommends not discarding any experiments outright. If experiments can be reinterpreted, assuming a new theory as basis, they may provide valuable additional insight.

One major problem within this field, however, is that while the literature provides a large amount of descriptive information on experimental observations in different zones, little or no information is provided to the reader on the importance of these different observations.

Connecting to this topic, George states that "the most attention-getting aspect of this debate has been about the validity of the log law or the power law alternative. Even those who still hold the classical views have been left in the uncomfortable position that **their 'universal' constants appear to be time-dependent, and vary from one experiment to the next**. But the new ideas have not been without their problems either. Some seem to work and be definitive, but other consequences of the same assumptions are less successful. To the casually interested on-looker and devoted researcher alike, the entire field appears to be in chaos." [4]

According to the new theory here proposed, the instability in the recorded log-law data and model constants, when looking more closely, are that *these experimental recordings all appear to be performed in large geometrical regions where the net kinetic energy dissipation is rather small* – perhaps 5% of net kinetic energy dissipation occurs in the log-law region according to present new model, a log-law region which practically spans most of the cross-section of a pipe. **Arguably, these instabilities connect directly with the very low kinetic energy dissipation rates per unit volume and are arguably to be considered as *secondary* phenomena.** Secondary phenomena are always much less stable to record in experiments, as compared to ***primary*** phenomena. It comes at no surprise to the author of the present work, that results obtained in measurements in the log-law region are rather unstable and vary from measurement to measurement.

This vexing problem with instabilities not only relates to experimental situations, but also to the here-proposed new theory. For instance:

- It is clearly more difficult to analyse accurately what occurs in zones of low rates of kinetic energy dissipation: For instance, the length L within the log-law region assumed to be around 1/6 of $L_{\max}$ in the viscous sub-layer region, appears speculative (see assumption in [6]).
- The assumption on the amount and range of the defect regions within the buffer zone and log-law region in Examples 1-2 in Section 3.4 appears speculative.
- The suggestions in Section 4 on how swirls may trigger, grow, and move into other zones and downstream behaviour, also appears to have small influence on the net kinetic energy dissipation rate and hence is admittedly speculative.

Despite these speculations and observed instabilities, secondary issues are here believed not to have very much influence on the stable results obtained in Table 1, and Figs. 3-4.

One aspect of the physics of the proposed new model, which is challenging to treat in a thermodynamic analysis, is the leakage of growing slips (and associated eddies) downstream.

In addition, the MEP process could mend defect zones utilizing the upstream-leaked slips (and associated eddies) – while the net kinetic energy dissipation across the cross-section of the pipe will slowly increase downstream.

These phenomena may suggest an overall slowly evolving transient behaviour of turbulence.

The experiments by [18] presents a situation of onset turbulence, which in long (smoothly polished) narrow pipes far downstream (from upstream-leaked slips) may reach a state in which the apparent turbulent behaviour ceases to exist – and instead form an apparent laminar flow situation.

In the context of present theory, perhaps one possible explanation of this transition from turbulence to a laminar flow situation indicates the accumulated effects of downstream mending – albeit the experiments performed by [18] showing a slowly evolving transient behavior would in turn indicate a rather small rate of mending to occur. Also, possibly, the mending might only occur in regions with relatively high kinetic energy dissipation rates.

It is of key interest to search for traces within experimental flow which may connect with the new proposed theory.

Regarding an MEP process, the author of the present work envisions a rather limited number of web fractures in the y_1-, y_2- and y_3-directions. Experimentally, there may be traces of behaviour in the rim of the turbulent side of a turbulent spot, where the presence of hair-pin vortexes might suggest a layered structure in the following downstream flow, possibly indicating a δ resolution within the viscous sublayer zone.

Also, consider the streamwise long streaks which "refer to narrow strips of low-momentum coherent motions extending lengthwise in the streamwise direction" [20] that exist within the viscous sublayer zone, an example of which is depicted in Fig. 23-8 (p. 717) in [1]. The spanwise (y_3-direction) gap between these are around 100-140 wall units. Could the presence of these streaks and the gap between them indicate an estimation of the length K of the flakes? (Perhaps the flakes are not perfectly in alignment with each other in the y_3-direction, while the possible differences in local y_2-direction flow – conceivably due to leakage or other fluctuation – could result in some vortex generation resulting in these streaks.) This is admittedly speculation. However, experimentally it appears that the same gap exists between these streaks all the way up the through the buffer- and log-law regions according to [20].

Also of speculative interest is the experimental observation of these streamwise streaks with equal gap width. They appear to have a length which is much longer in the viscous sublayer as compared to the corresponding length in the log-law region [20]. Again, this triggers additional speculation as to whether there may be a connection between the lengths of these long streaks and the parameter L, which varies similarly from the viscous sublayer region up through the buffer- and log-law region.

For future work, it would be of interest to estimate a minimum δ within the viscous sublayer. What key parameters would control this thickness, and what is the kinetic energy dissipation "saturation" level? Is there a connection to kinetic theory of gases and mean-free paths?

Finally, to comment on the arguably most important zone, namely the viscous sub-layer, the author has utilized the best-available knowledge on the velocity profile across this layer, which in turn is based on the original scaling laws and experimental results dating back to the 1930's. A peculiarity that needs addressing is one of possible inconsistency:

The law of the wall for the viscous sublayer region states a relationship ${U_1}^+ = {y_2}^+$ to be approximately valid. What this relationship really presents is a reformulation of the correlation between shear stress and strain rate: $U_1/U^* = y_2U^*/\nu$, or $U_1 = y_2(U^*)^2/\nu$, or $U_1 = y_2\tau/\mu$, which gives upon differentiation with y_2: $\mu(\partial U_1/\partial y_2) = \tau$, which in turn is the well-known fundamental model valid for viscous laminar flows.

According to Section 3.6, a different slope might be present – however with an approximately constant velocity gradient throughout this viscous sublayer region.

However, arguably **the rather fair results on the turbulence onset and present at-face agreement would suggest that the velocity slope in the viscous sublayer is not too different from the original assumptions made in the 1930s**.[2] Also, it is difficult to challenge the carefully performed mean-flow velocity experiments, although the literature has presented the viscous sublayer thickness in rather approximative numbers: Indeed, if the velocity recorded accurately in the interface between viscous sublayer and buffer layer, and the distance to the wall is accurately recorded, then a result close to ${U_1}^+ = {y_2}^+$ throughout the viscous sublayer region would be difficult to contest.

It is interesting to observe scientists recently placing more attention on experimentally recording the velocity profile across the viscous sublayer zone, *cf. e.g.* [21].

The renewed recent experimental focus on the viscous sublayer is very welcome, in the context of present work, where this zone is arguably the most important zone as

[2] Several physical reasons may contribute to the apparent finding $C_{\text{vs}} \approx 1$. For instance: (a) Between the flakes in the non-slip interfaces, one may assume fluid to exist, possibly with a no-slip line-wise contact with a solid wall. (b) The proposed residual slip-flow processes do not significantly change the local density of the fluid.

regards to net kinetic energy dissipation and contribution to the skin friction.

6 Conclusions

On the matter of turbulence onset and offset, it was demonstrated here how the nominal model in [6] can be adjusted to obtain more realistic transition Re numbers for pipe flow while accounting for the surface roughness. As the nominal model of [6] indicated a transition point at Re numbers around 870-975, it was demonstrated that an approximately 50% higher flow gradient assumed on the laminar flow side – as a result of a suction process in a turbulent spot – appears to improve the estimated onset transition Re number (to around Re=2300).

In sum, the present results combine the remarkably high kinetic energy dissipation rate occurring in the viscous sublayer, with onsets predicted (based on the conditions inside the viscous sublayer) at Re numbers in fair agreement with experiments using a nominal transition model, and at Re numbers in close agreement with experiments using a slightly adjusted transition model. The remarkably high kinetic energy dissipation concentrated near- and in the vicinity of the wall implies that little or almost no effects on the net kinetic energy dissipation as a result of the large-scale turbulent eddy motion can be found – and hence the need to adopt computationally-intense flow solvers can be questioned.

On the matter of adopting the present new theory in CFD flow solvers, the findings made here amount to good news for the modeller concerned with turbulent skin friction computations, on the prospect of working generally with a perfect web fracture structure. The modeller no longer has to worry too much about the differences between the defect web and the perfect web, or the transient simulation of eddies.

However, for the study of mixing, boundary-layer thickness, or wall-pressure fluctuations, it can be noted that the discrete framework of residual thermodynamics [12] allows for the utilizing of "apparent material properties", *i.e.* a corresponding continuum model formulation derived from a discrete process formulation, which implies possibilities to adapt the present theory to a CFD flow solver.

Acknowledgements:

This work was supported by Hot Disk AB (Sweden). Special thanks to D.Sc. S.E. Gustafsson at Dept. Physics, Chalmers Univ. of Technology, Dr. H. Otterberg at University of Gothenburg, Assoc. Prof. J. Gustavsson and Prof. Å. Haglund at Dept. Microtechnology & Nanoscience, Chalmers Univ. of Technology, as well as Ms. B. Lee at Hot Disk AB (Sweden), for assistance in preparing this manuscript.

Nomenclature

b, B	functions used in dimensionless scaling
c	speed of sound in fluid (m s^{-1})
C^+, C^{++}	log-law intercept on U^+- or U^{++}-axis, respectively (-)
C_A	model constant (m s^{-2})
C_{vs}	model constant (-)
D	diameter of pipe interior (m)
K	width of flake (in y_3-direction) (m)
$\frac{\mathrm{d(KE)}}{\mathrm{d}t}$	total kinetic energy dissipation rate (W)
$\frac{\mathrm{d(ke)_{res}}}{\mathrm{d}t}$	kinetic energy dissipation rate per unit volume, due to residual process (W m^{-3})
$\frac{\mathrm{d(ke)_{viscous}}}{\mathrm{d}t}$	viscous dissipation rate for viscous laminar flows of Newtonian fluids, per unit volume (W m^{-3})
$\frac{\mathrm{d(ke)}}{\mathrm{d}t}$	kinetic energy dissipation rate per unit volume (W m^{-3})
f	Darcy friction factor (-)
L	slip length of flake fracture (m)
M	Mach number, where $M = U_{\mathrm{mean}}/c$ in pipe flow computations (-)
o, O	functions used in dimensionless scaling
R	radius of pipe interior (m)
r	radial distance from centerline (m)
Re	Reynolds number (-)
U	Velocity (m s^{-1})
U_i	Cartesian component i of velocity vector (m s^{-1})
U_{max}	Maximum velocity (m s^{-1})
U_{mean}	Mean (average) velocity (m s^{-1})
U_{slip}	slip velocity (m s^{-1})
U^*	Friction velocity (m s^{-1})
y_1, y_2, y_3	Cartesian co-ordinates (m)

Greek letters

γ	boundary layer thickness (m)
δ	gap width between slip layers, also referred to as thickness of flake fracture, or resolution parameter (m)
ε	surface roughness (m)
κ	von Kármán constant $(-)$
μ	dynamic viscosity of Newtonian fluid (kg m^{-1} s^{-1})
ν	kinematic viscosity of the Newtonian fluid (m^2 s^{-1})
ρ	density (kg m^{-3})
τ	shear stress (N m^{-2})

Subscripts

bl	for buffer layer
max	maximum
min	minimum
outer,max	referring to position at edge of outer layer
res	for residual process
vs	for viscous sublayer
wall	wall position

Special notations

$\frac{\mathrm{d}}{\mathrm{d}t}$	time derivative (s^{-1})
$(\cdot)^+$	dimensionless scaling for fixed log-law intercept C^+, with fixed range in $y_2{}^+$ for viscous sublayer, buffer layer and log-law regions (*cf.* Fig. 2) (traditional scaling).
$(\cdot)^{++}$	dimensionless scaling for a variable log-law intercept, with variable range in $y_2{}^+$ for viscous sublayer, buffer layer and log-law regions (*cf.* Fig. 8 in [6]) – depending on the wall surface roughness.

References:

[1] R.L. Panton, *Incompressible Flow*, John Wiley & Sons, New York, USA, 1984.

[2] H. Tennekes, J.L. Lumley, *A First Course in Turbulence*, MIT Press, 1972.

[3] C. Liu, P. Lu, L. Chen, Y. Yan, "New Theories on Boundary Layer Transition and Turbulence Formation", *Modelling and Simulation in Engineering*, Article ID 619419, 2012.

[4] W.K. George, "Recent Advancements Toward the Understanding of Turbulent Boundary Layers", *American Institute of Aeronautics and Astronautics* Paper AIAA-2005-4669.

[5] F.M. White, *Fluid Mechanics*, 2nd Ed., McGraw-Hill Book Company, 1986.

[6] M. Gustavsson, "A Residual Thermodynamic Analysis of Turbulence – Part 1: Theory", *submitted for publication*.

[7] H.W. Emmons, "The laminar-turbulent transition in a boundary layer – Part I", *J. Aero. Sci.* 18, 490–498, 1951.

[8] H.W. Emmons, A.E. Bryson, "The laminar-turbulent transition in a boundary layer (Part II)", *Proc. 1st US Natl. Cong. Appl. Mech.*, 859–868, 1952.

[9] S.H. Davis, J.L. Lumley (eds.), *Frontiers in Fluid Mechanics: A Collection of Research Papers Written in Commemoration of the 65th Birthday of Stanley Corrsin*, Springer Verlag, 1985.

[10] P. Jonáš, "On the Turbulent Spot and Calmed Region", Engineering Mechanics 2007, National Conference with International Participation, Svratka, Czech Republic, May 14-17, 2007.

[11] K. Sreenivasan, P.A. Davidson, Y. Kaneda, K. Moffatt, *A Voyage Through Turbulence*, Cambridge University Press, 2011.

[12] M. Gustavsson, ''Residual Thermodynamics: A Framework for Analysis of Non-Linear Irreversible Processes'', *Int. J. Thermodynamics*, *15*, 69–82, 2012.

[13] K. Narahari Rao, R. Narasimha, M.A. Badri Narayanan, "The 'Bursting' Phenomenon in A Turbulent Boundary Layer", *J. Fluid Mech. 48*, 339-352, 1971.

[14] D. Ross, J.M. Robertson, "Shear Stress in a Turbulent Bounday Layer", *J. Appl. Phys.* 21, 557-561, 1950.

[15] F. Schultz-Grunow, "Über das Nachwirken der Turbulenz bei Örtlich und Zeitlich Verzögerter Grenzschichtströmung", *Proc. 5th Int. Cong. Appl. Mech.*, Cambridge, Massachusetts, 428-435, 1938.

[16] W. Jacobs, *Zeit. f. angew. Math. u. Mech.* 19, 1939. Translated in NACA Tech. Memo 951 (1940).

[17] D. Lathrop, "Turbulence Lost in Transience", *Nature* 443**,** 36–37, 2006.

[18] B. Hof, J. Westerweel, T.M. Schneider, B. Eckhardt, "Finite Lifetime of Turbulence in Shear Flows", *Nature* 443, 59–62, 2006.

[19] D. Vergano, "Turbulence theory gets a bit choppy", *USA Today*, September 10, 2006.

[20] W. Wang, C. Pan, J. Wang, "Wall-Normal Variation of Spanwise Streak Spacing in Turbulent Boundary Layer With Low-to-Moderate Reynolds Number", *Entropy* 21, p. 24-, 2019

[21] J. K. Abrantes, "Holographic Particle Image Velocimetry for Wall Turbulence Measurements", Ph.D. thesis, Ecole Centrale de Lille, 2012.